

# A New Family of ZVS-PWM Active-Clamping DC-to-DC Boost Converters: Analysis, Design, and Experimentation

Cláudio Manoel da Cunha Duarte, *Student Member, IEEE*, and Ivo Barbi, *Senior Member, IEEE*

**Abstract**—The purpose of this paper is to introduce a new family of zero-voltage switching (ZVS) pulse-width modulation (PWM) active-clamping dc-to-dc boost converters. This technique presents ZVS commutation without additional voltage stress and a significant increase in the circulating reactive energy throughout the converters. So, the efficiency and the power density become advantages when compared to the hard-switching boost converter. Thus, these converters may become very attractive in power factor correction applications. In this paper the complete family of boost converters is shown, and one particular circuit, taken as an example, is analyzed, simulated, and experimented. Experimental results are presented, taken from a laboratory prototype rated at 1600 W, input voltage of 300 V, output voltage of 400 V, and operating at 100 kHz. The measured efficiency at full load was 98%, and the converter kept an efficiency up to 95% from 17% to 100% of full load, without additional voltage and current stresses.

**Index Terms**—Active clamping, dc-to-dc converters, soft commutation.

## I. INTRODUCTION

THE BOOST converter, as a preregulator, in ac-to-dc high power factor and low total harmonic distortion (THD) power supplies, has shown to be the best choice for single-phase rectification. Thus, this converter has played an important role in the power electronics area, and it has been the subject of incessant studies in the search of better efficiency and lower weight and volume.

Through the synthesis technique of clamped mode dc-to-dc converters topologies, presented in [1], it was possible to generate six different circuits of boost converters. These circuits are presented and studied hereafter.

Fig. 1 shows the six boost converters. In all of them the power transferred to the load is by a boost stage, while the clamping action is by a buck stage, shown in Fig. 1(a), a boost stage in Fig. 1(b), a buck-boost stage in Fig. 1(c), a Cuk stage in Fig. 1(d), a SEPIC stage in Fig. 1(e), and a zeta stage in Fig. 1(f). So, these converters will be called by boost-buck, boost-boost, boost-buck-boost, boost-cuk, boost-sepic, and boost-zeta.

These converters differ from a conventional boost pulse-width modulation (PWM) converter by an additional auxiliary switch ( $S_2$ ), one or two resonant inductor ( $L_{r1}, L_{r2}$ ), a

resonant capacitor ( $C_r$ ), which includes the output capacitance of the power switches, and one or two clamping capacitor ( $C_{c1}, C_{c2}$ ) where  $S_1$  is the main switch.

## II. OPERATION AND ANALYSIS OF THE CLAMPED MODE ZVS-PWM BOOST CONVERTER WITH THE CLAMPING ACTION BUCK-BOOST

### A. Principle of Operation

To simplify the analysis, the input filter inductance is assumed large enough to be considered as a current source ( $I_s$ ). The capacitor ( $C_c$ ) is selected to have a large capacitance so that the voltage  $V_c$  across the capacitor  $C_c$  could be considered as a constant one. The six topological stages and key waveforms of the boost-buck-boost converter to one switching cycle are shown in Figs. 2 and 3. In those figures it can be seen that the two switches are switched in a complementary way. The main switch ( $S_1$ ) is turned off at  $t = t_0$ , when the switching period starts.

Prior to  $t_0$ , the main switch ( $S_1$ ) is on and the auxiliary switch is off. When  $S_1$  is turned off at  $t = t_0$ , the capacitor  $C_r$  is linearly charged, by  $I_s$ , to  $V_0$ . Due to the presence of  $C_r$ ,  $S_1$  is turned off with no switching loss. Then  $V_{Cr}$  reaches  $V_0$ , the boost diode ( $D_b$ ) starts conducting. The current through  $L_r$  and  $V_{Cr}$  evolves in a resonant way, and  $V_{Cr}$  rises from  $V_0$  up to  $V_c + V_0$ . After that, the voltages are clamped. As  $V_{Cr}(t) = V_c + V_0$ , the voltage across  $S_2$  is zero, thus  $S_2$  turns on with no losses zero-voltage switching (ZVS). The  $L_r$  current ramps down until it reaches zero, when it changes its direction and rises again. This stage ends when  $S_2$  is turned off at  $t = t_3$ . The voltage across  $C_r$  falls, due to the resonance between  $L_r$  and  $C_r$ , until it reaches zero at  $t = t_4$ . In stage 5,  $S_1$  is turned on with no switching losses (ZVS), because  $V_{Cr}$  became null. The current through  $L_r$  changes its polarity and ramps up to reaches  $I_s$ . At  $t = t_5$ , the diode  $D_b$  becomes reversibly biased and power is not transferred to the load. This stage ends when  $S_1$  is turned off at the end of the switching cycle.

### B. DC Voltage Conversion Ratio and DC Voltage Clamping Ratio

As the time intervals  $\Delta t_1$ ,  $\Delta t_2$ , and  $\Delta t_4$  are very short in relation to the switching cycle, they will not be considered in this analysis. Thus, let us consider the waveform shown in Fig. 4.

Manuscript received July 3, 1996; revised November 25, 1996. Recommended by Associate Editor, J. Suozzi.

The authors are with the Federal University of Santa Catarina, INEP, 88040-970 Florianópolis, SC, Brazil.

Publisher Item Identifier S 0885-8993(97)06401-6.

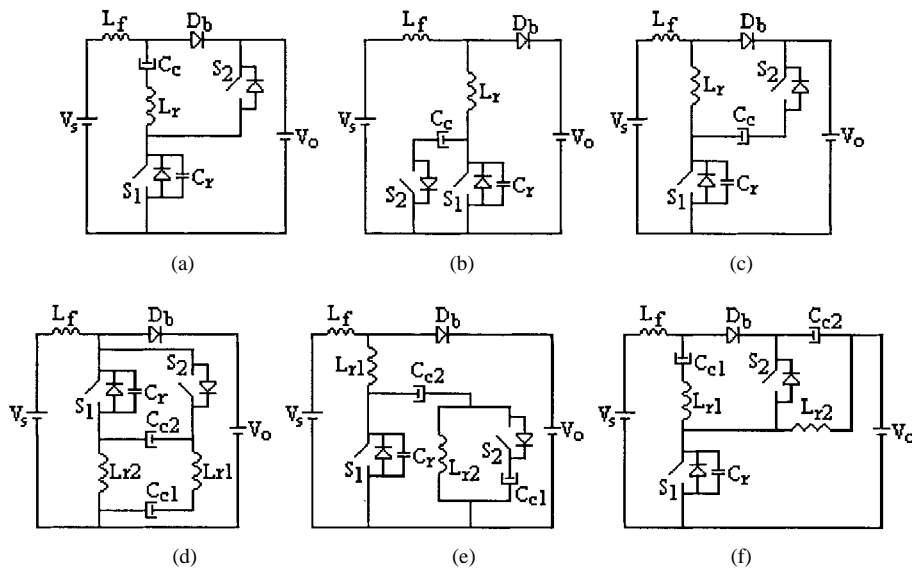


Fig. 1. ZVS-PWM active clamping boost converters: (a) Boost-buck. (b) Boost-boost. (c) Boost-buck-boost. (d) Boost-cuk. (e) Boost-sepic. (f) Boost-zeta.

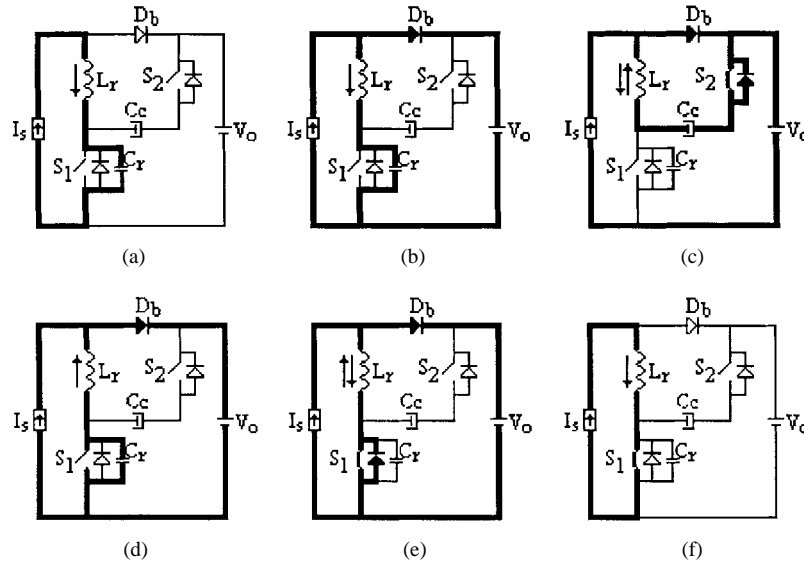


Fig. 2. Topological stages assumed by boost-buck-boost converter.

The power that flows in the clamping capacitor must be zero in a switching cycle for the operation to be steady. The voltage across \$C\_c\$ is constant, so its average current must be zero. Thus

$$\int_0^{(1-D)T_s} \left[ \frac{-V_c}{L_r} t + I_s \right] dt = 0 \tag{1}$$

then

$$\beta = \frac{V_c}{V_0} = \frac{2L_n}{(1-D)} \tag{2}$$

$$\frac{V_{Spk}}{V_0} = \beta + 1 = 1 + \frac{2L_n}{(1-D)} \tag{3}$$

$$q = \frac{V_0}{V_s} = \frac{1}{1 - [D - 2L_n]} \tag{4}$$

where

$$L_n = L_r \frac{I_s}{V_0 T_s} = L_r \frac{I_0}{V_s T_s} \tag{5}$$

and \$V\_{Spk}\$ is the maximum voltage across \$S\_1\$ and \$S\_2\$.

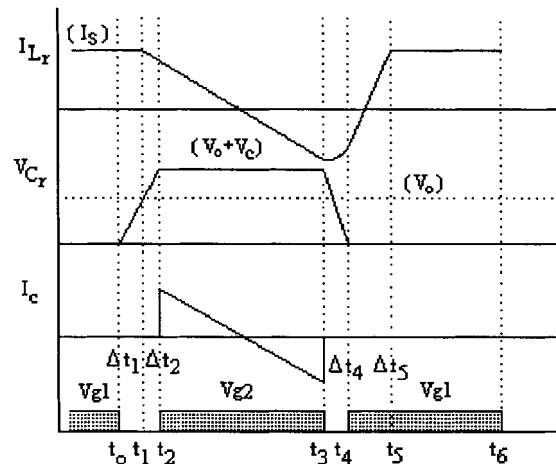
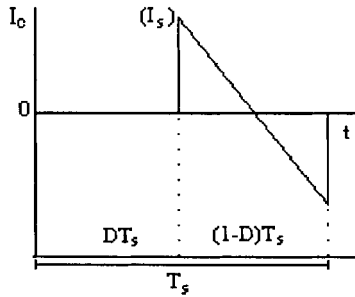


Fig. 3. Relevant ideal waveforms.

Fig. 4. Current through  $C_c$ .

The dc voltage clamping ratio given by (3) is graphically represented in Fig. 5(a), and the dc voltage conversion ratio (q) is shown in Fig. 5(b) for different duty cycles (D).

### C. Commutation Analysis

Due to the capacitance  $C_r$ ,  $S_1$  and  $S_2$  are turned off with no losses, in a ZVS way. However,  $S_1$  and  $S_2$  will turn on with no losses, only if there is enough energy stored in  $L_r$  to achieve soft commutation. At  $t = t_1$ , it is necessary to charge  $C_r$  from  $V_0$  to  $V_c$ . At  $t = t_3$ , it is necessary to discharge  $C_r$  from  $V_c + V_0$  to zero. The latter is more difficult because it needs more energy. Thus, if enough energy is guaranteed to achieve soft commutation for  $S_1$ , then  $S_2$  will achieve soft commutation too. Thus, from energy relationships in  $L_r$  and  $C_r$ , at  $t = t_3$ , we have

$$L_n \geq \frac{(1-D)}{(1-D)f-2} \quad (6)$$

where

$$f = \frac{f_0}{f_s}. \quad (7)$$

As that result was achieved on a model with imposed current, then, at  $t = t_3$ , the current through  $L_r$  is equal to the average input current. But, in the real prototype, there is an input inductor that has maximum current greater than average current, so there is more energy stored to commutation. Thus, (6) must have a correction factor, which is represented in (8)

$$L_{n_{\min}} = \frac{1}{\pi f(2+r) - \frac{2}{(1-D)}} \quad (8)$$

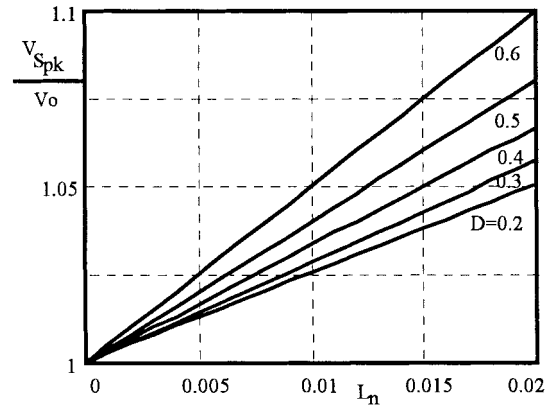
where ( $r$ ) is the percentage input current ripple

$$r = \frac{\Delta I_s}{I_s} \quad (9)$$

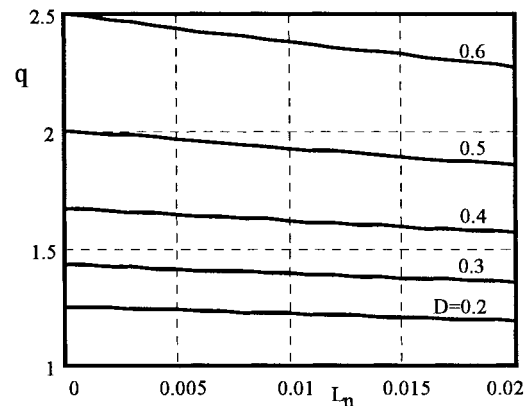
and, if the efficiency were considered, the expression becomes

$$L_{n_{\min}} = \frac{\eta}{\pi f(2+r) - \frac{2}{(1-D)}}. \quad (10)$$

From the analysis before, it is clear that soft commutation, when  $S_1$  turns on, will be achieved depending on  $I_s$  and  $L_r$ . And, as  $I_s$  depends on the processed power, then that commutation will occur with no losses, only in a range of load that will be established through (8). But although that



(a)



(b)

Fig. 5. Boost-boost, boost-buck-boost, boost-cuk and boost-sepic: (a) theoretical dc voltage clamping ratio across switches; (b) theoretical dc voltage conversion ratio.

commutation is not completely without losses, the converter will still operate with high efficiency in light load situations, because there will always be enough energy stored in  $L_r$  to help the commutation process, and the lost energy never will be so high, as in a completely hard commutation.

As the critical commutation is when  $S_1$  turns on, it is important to determine the time interval between the turning on of  $S_1$  and turning off of  $S_2$ . This time interval is necessary for the existence of soft commutation. Then

$$t_d = \frac{(V_0 + V_c)}{2I_s} C_r + \frac{I_s}{2V_0} L_r. \quad (11)$$

### D. Voltage and Current Stresses on Switches

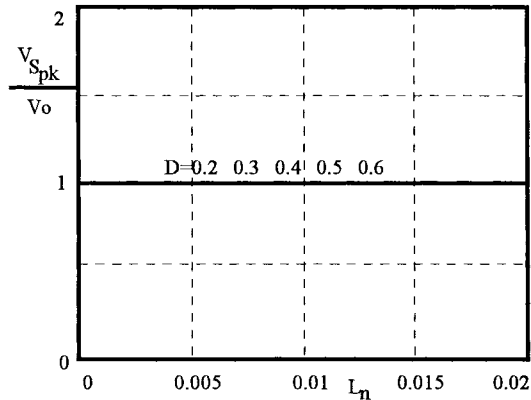
The voltage and current stresses on switches are presented in Table I. All current and voltages are normalized in relation to  $I_s$  and  $V_0$ .

## III. RELEVANT ANALYSIS RESULTING FROM THE ENTIRE FAMILIES OF CONVERTERS

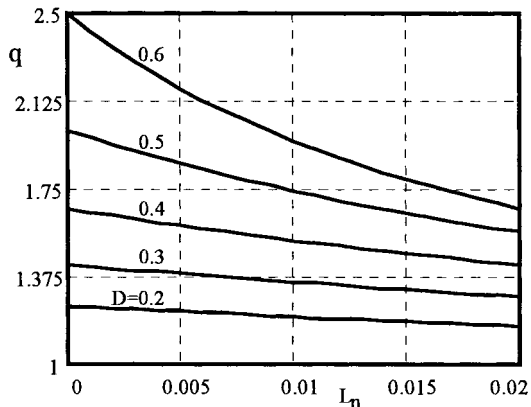
All the converters were analyzed and it was possible to arrive at some conclusions by comparing their performances. Shown below, in Figs. 6 and 7, are the dc voltage clamping ratios across the switches and the dc voltage conversion ratio, for boost-buck and boost-zeta converters, while the other converters, are shown in Fig. 5.

TABLE I  
CURRENT AND VOLTAGE STRESSES ON SWITCHES  
FOR BOOST-BUCK-BOOST CONVERTER

	Switch $S_1$	Switch $S_2$	Diode $D_b$
$V_{\max}$	$1 + \frac{2L_n}{(1-D)}$	$1 + \frac{2L_n}{(1-D)}$	1
$I_{pk}$	1	1	2
$I_{rms}$	$\sqrt{D - \frac{4}{3}L_n}$	$\sqrt{\frac{(1-D)}{3}}$	$\sqrt{\frac{2}{3}(1-D) + 4L_n}$
$I_{avg}$	$D - 2L_n$	0	$1 - (D - 2L_n)$



(a)

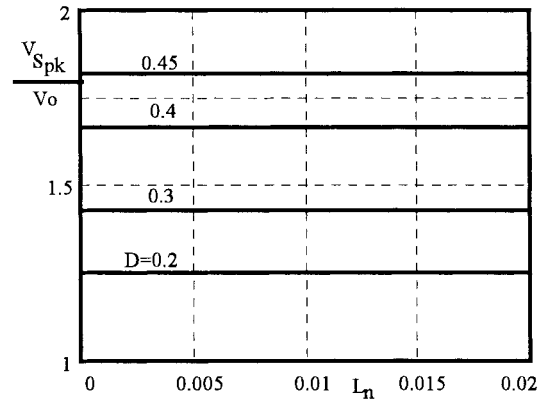


(b)

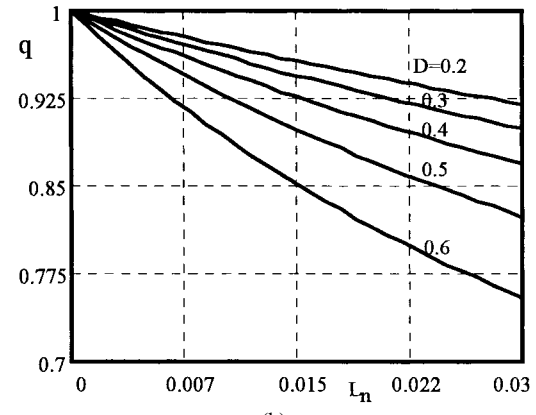
Fig. 6. Boost-buck converter: (a) theoretical voltage clamping ratio across switches; (b) theoretical output characteristics.

Although the boost-boost, boost-buck-boost, boost-cuk, and boost-sepic converters present the same external characteristics and the same voltage clamping on switches, conceptually they are different, and present different voltages across the clamping capacitor.

Through the analysis it was proved that the boost-buck converter presented lower voltage stress on switches, but higher current stress, and its clamping capacitor is under all load current, which is a disadvantage. The boost-zeta converter presented the worst performance, because has higher current and voltage stresses on switches, and less efficiency than the others. From that analysis, one can conclude that the



(a)



(b)

Fig. 7. Boost-zeta converter: (a) theoretical voltage clamping ratio across switches; (b) theoretical output characteristics.

buck-boost clamping action, is the best for boost converters applications.

#### IV. DESIGN EXAMPLE

In this Section, a design example for the boost-buck-boost converter will be presented. The specifications are as follows:

$$V_s = 300 \text{ V (input voltage)}$$

$$V_o = 400 \text{ V (output voltage)}$$

$$P_{out} = 1600 \text{ W and } f_s = 100 \text{ kHz.}$$

The efficiency must be kept high from light load conditions to full load. Therefore, the load range with soft commutation in the main switch ( $S_1$ ) will be established from 55% to 100% of full load. From the specifications it is possible to achieve the dc voltage-conversion-ratio, given by

$$q = \frac{V_o}{V_s} = \frac{400}{300} = 1.333.$$

Throughout the dc voltage-conversion-ratio and the output characteristics, shown in Fig. 5(b), are obtained the nominal duty cycle, the normalized resonant inductance and the resonant inductance. The determination of those parameters results in the establishment of the operation point, and in the range of load with soft commutation in  $S_1$ . Although it is important to consider that the greater the value of  $L_r$ , the greater will be the range of load with soft commutation in  $S_1$  which results in greater clamping voltage.

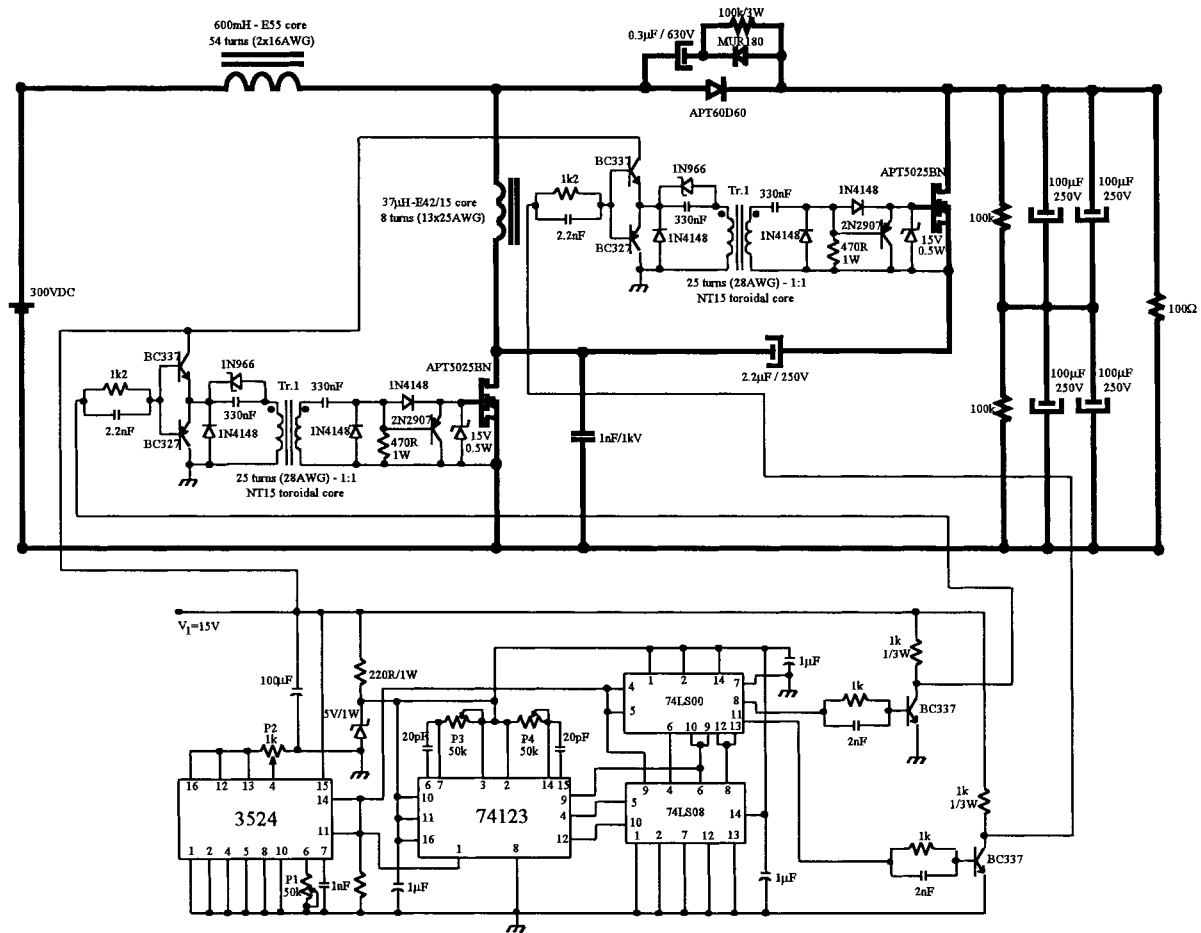


Fig. 8. Complete circuit of the implemented prototype.

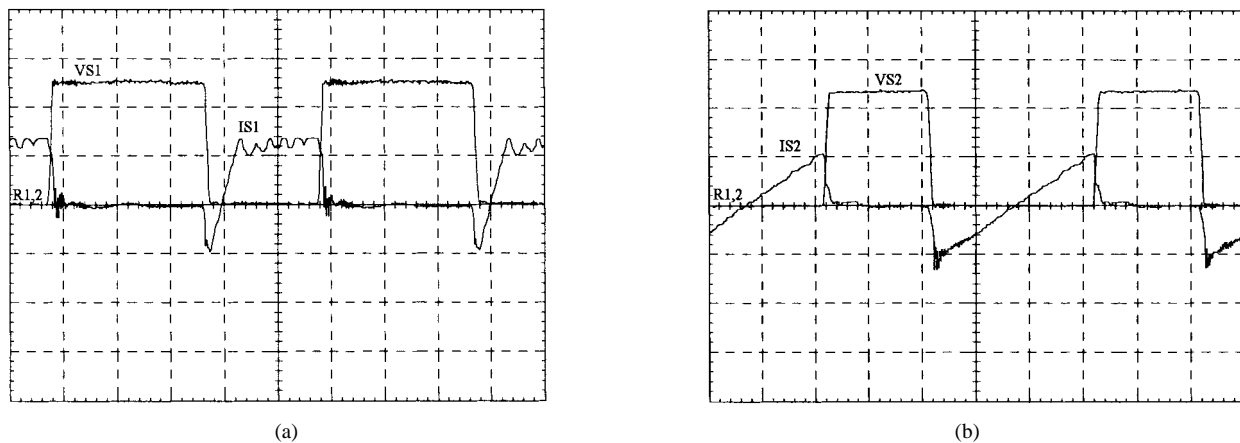


Fig. 9. (a) Drain-to-source voltage across  $S_1$  and current through  $S_1$  and  $C_r$ . (b) Drain-to-source voltage across  $S_2$  and current through  $S_2$ ; (voltage: 200 V/div; current: 5 A/div; time scale: 2  $\mu$ s/div).

As a closed solution in this case would be difficult to achieve, it is necessary to do some interactions to obtain the desired operation point, and the range of load with soft commutation in  $S_1$ . So, it is necessary to determine the values of  $D, L_n, L_r$ , and  $C_r$ , and then, to verify if the load of range with soft commutation in  $S_1$ , is that desired. If it is less than that desired, the value of  $L_r$  must be increased. Then, with

$q = 1.333$ , and choosing  $D = 0.302$ , through Fig. 5(b), it has  $L_n = 0.0519$ , and from Fig. 5(a), results

$$\frac{V_{Spk}}{V_0} = 1.1487 \quad \beta = 0.1487.$$

Thus, we have

$$L_r = \frac{L_n V_0}{f_s I_s} = 37 \mu\text{H}.$$

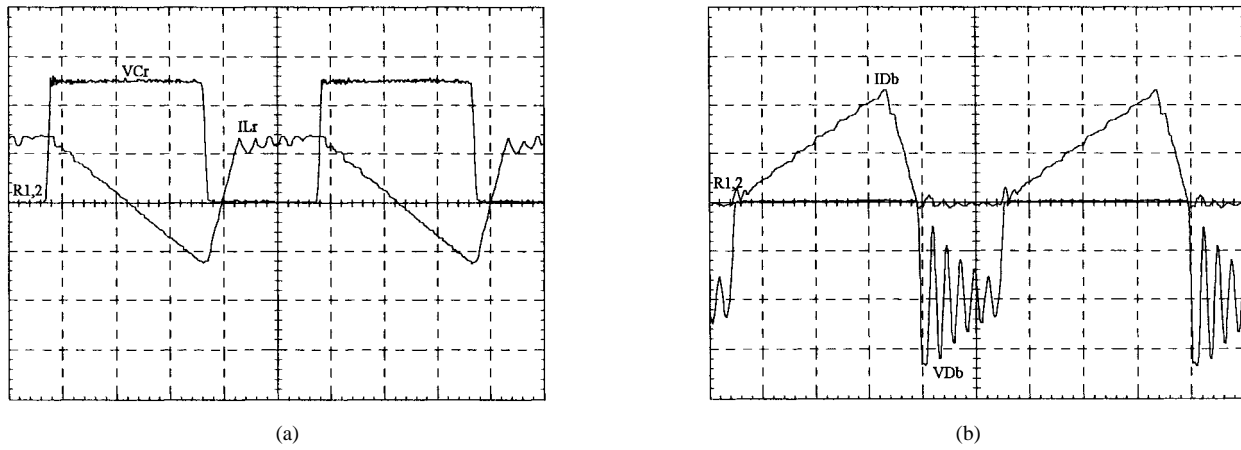


Fig. 10. (a) Voltage across  $C_r$  and current through  $L_r$ ; (b) voltage across  $D_b$  and current through  $D_b$ ; (voltage: 200 V/div; current: 5 A/div; time scale: 2  $\mu$ s/div).

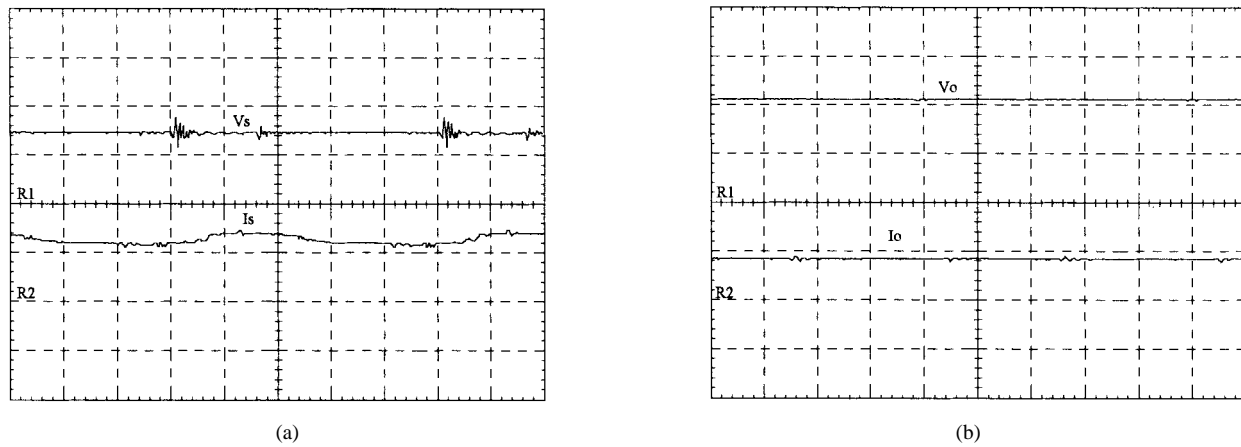


Fig. 11. (a) Input voltage and current; (b) output voltage and current; (voltage: 200 V/div; current: 5 A/div; time scale: 2  $\mu$ s/div).

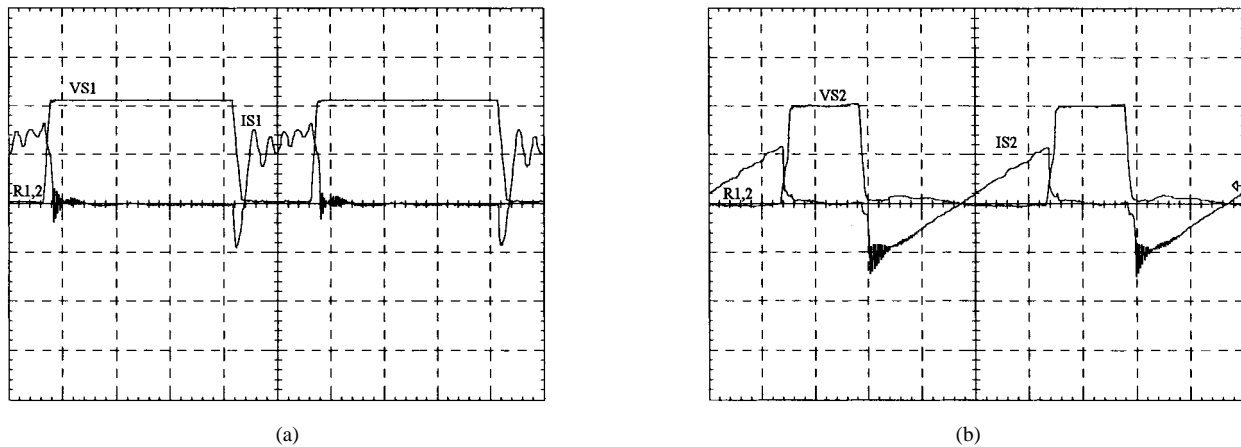


Fig. 12. (a) Drain-to-source voltage across  $S_1$  and current through  $S_1$  and  $C_r$ . (b) Drain-to-source voltage across  $S_2$  and current through  $S_2$ ; (voltage: 200 V/div; current: 2 A/div; time scale: 2  $\mu$ s/div).

The resonant frequency, of the circuit  $L_r$  and  $C_r$ , must be much higher than the switching frequency so the commutations become a small part of the switching period. Then,  $f = 5.28$  has been chosen. So

$$2\pi f_0 = \frac{1}{\sqrt{L_r C_r}} \Rightarrow C_r = 2.46 \text{ nF.}$$

As the input current ripple is taken by 24% of the average input current, and the efficiency is considered as 95%, this results in

$$L_{n\min} = \frac{0.95}{\pi \cdot 5.28 \cdot (2 + 0.24) - \frac{2}{(1 - 0.302)}} = 0.027645.$$

Then, as  $L_{n\min} = 0.5327L_n$ , a range of load with soft

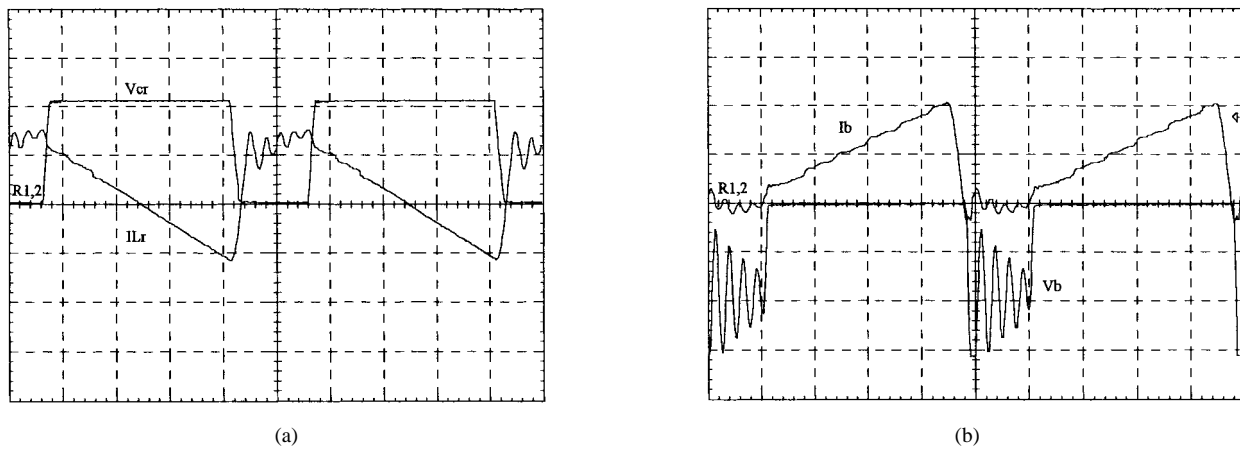


Fig. 13. (a) Voltage across  $C_r$  and current through  $L_r$ ; (b) voltage across  $D_b$  and current through  $D_b$ ; (voltage: 200 V/div; current: 2 A/div; time scale: 2  $\mu$ s/div).

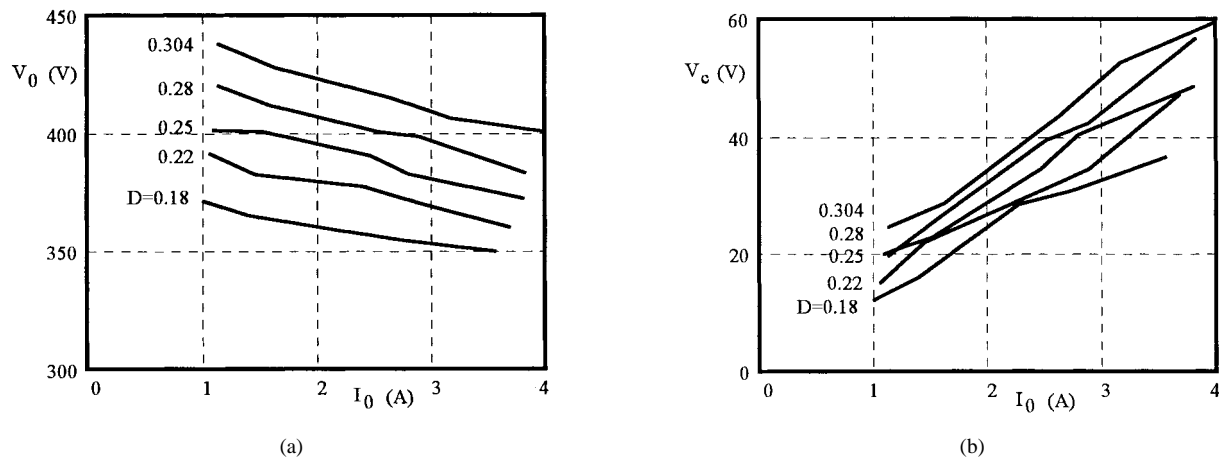


Fig. 14. (a) Output voltage with different load conditions and duty cycle. (b) Voltage across the clamping capacitor with different load conditions and duty cycle.

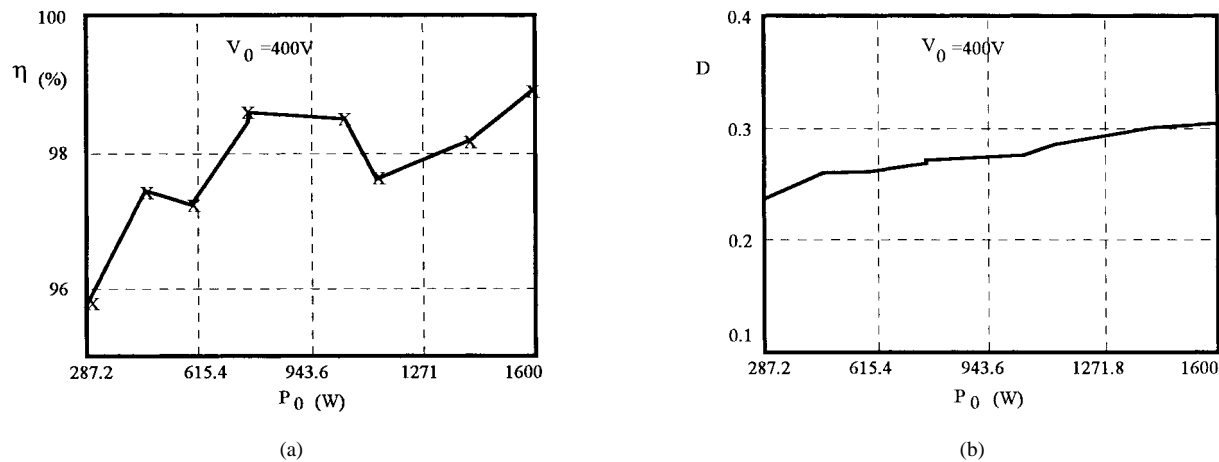


Fig. 15. (a) Experimental efficiency curve with constant output and input voltage. (b) Duty cycle variation to keep output voltage constant with different load conditions.

commutation in  $S_1$  from 53.27% to 100% of full load is obtained, which satisfy the specified value (from 55% to 100%). The time interval between the turning on of  $S_1$  and the turning off of  $S_2$  is

$$t_d = \left[ \frac{0.45948}{2 \cdot 5.61} \cdot 2.46 + \frac{5.61 \cdot 37 \cdot 10^{-6}}{2 \cdot 400} \right] 10^{-6} \cong 360 \text{ ns.}$$

### V. EXPERIMENTAL RESULTS

Following the same design outlined in the preceding section, a boost ZVS-PWM converter with buck-boost clamping action (boost-buck-boost) was implemented, with the following specifications:

- 1) output power  $P = 1600$  W;
- 2) input voltage  $V_s = 300$  V;

- 3) output voltage  $V_0 = 400$  V;
- 4) switching frequency  $f_s = 100$  kHz.

The complete circuit diagram of the converter is shown in Fig. 8. The power stage consists of the following parameters:

- 1) switches  $S_1$  and  $S_2$ : Power MOSFET's APT5025;
- 2) diode  $D_b$ : APT60D60;
- 3) external resonant capacitor  $C_{\text{rext}}$ : 1000 pF/1.6 kV;
- 4) clamping capacitor  $C_c$ : 2.2  $\mu$ F/200 V;
- 5) output filter capacitor  $C_f$ : 100  $\mu$ F/250 V;
- 6) resonant inductor  $L_r$ : 37  $\mu$ H, core (E-45/15)-Thornton;
- 7) input filter inductor  $L_f$ : 600 mH, core (E-55) Thornton.

Experimentally obtained waveforms of the switches current and drain-to-source voltages are shown in Fig. 9. The resonant inductor current and voltage across the resonant capacitor are shown in Fig. 10(a), while the current through the diode  $D_b$  and the voltage across that diode are shown in Fig. 10(b). Fig. 11(a) and (b) shows the input and output voltage and current, respectively. These waveforms agree with those predicted theoretically, and as can be noted from the waveforms shown in Fig. 9, the main switches ( $S_1$  and  $S_2$ ) present ZVS commutation and its voltages are clamped at a specified value.

The load range with integral soft commutation in  $S_1$ , obtained experimentally, was from 48.5% to 100% of full load. In Figs. 12 and 13, are shown the main waveforms with 48.5% of full load. As we can see, integral soft commutation is obtained for both switches  $S_1$  and  $S_2$ . For loads less than 48.5% of full load,  $S_1$  will start to turn on with some losses, but the level of energy evolved in that commutation will be very low, which will not affect significantly the converter efficiency. Then, as  $S_2$  will always switch without losses the converter will operate with high efficiency, even in light load situations.

In Fig. 14(a), the output voltage as a function of output current is shown, for different duty cycles, and in Fig. 14(b), the voltage across clamping capacitor for the same conditions can be noted. The experimental efficiency curve of the converter, is shown in Fig. 15(a), while the duty cycle necessary to keep the output voltage in 400 V, is shown in Fig. 15(b). The converter presented high efficiency (up to 95%) from 17.95% to 100% of full load.

## VI. CONCLUSION

This paper presented a new family of ZVS-PWM active-clamping dc-to-dc boost converters. The boost with buck-boost clamping action, boost-buck-boost, converter was analyzed as an example. Theoretical studies and experimental results, allow us to draw the following conclusions.

- 1) Soft commutation (ZVS) is achieved for the active switches without notable voltage and current stresses.
- 2) The converters are regulated by the conventional PWM technique at constant frequency.
- 3) High efficiency was obtained from light load to full load.

The new converters are suitable for power factor correction rectifiers, particularly for 1.6-kW power supplies, where MOSFET's can be used, without increasing of conduction losses.

## REFERENCES

- [1] C. M. C. Duarte and I. Barbi, "A family of ZVS-PWM active-clamping dc-to-dc converters: Synthesis, analysis, and experimentation," in *Proc. Int. Telecommun. Energy Conf.*, 1995, pp. 502-509.
- [2] B. Carsten, "Design techniques for transformers active reset circuits at high frequencies and power levels," in *Proc. High Frequency Power Conversion*, 1990, pp. 235-246.
- [3] R. Watson, F. C. Lee, and G. C. Hua, "Utilization of an active-clamp circuit to achieve soft switching in flyback converters," in *Proc. IEEE Power Electron. Specialists Conf.*, 1994, pp. 909-916.
- [4] K. Harada and H. Sakamoto, "Switched snubber for high frequency switching," in *Proc. IEEE Power Electron. Specialists Conf.*, 1990, pp. 181-188.



**Cláudio Manoel da Cunha Duarte** (S'94) was born in Pelotas, Rio Grande do Sul, Brazil, in 1960. He received the B.S. degree in 1982 from the Catholic University of Pelotas-UCPel, Pelotas (RS), Brazil, and the M.S. degree in 1993 from the Federal University of Santa Catarina, Florianópolis (SC), Brazil, both in electrical engineering. He is currently working toward the Ph.D. degree in electrical engineering at the Power Electronics Institute of Federal University of Santa Catarina.

From August 1983 to early 1994, he was Assistant Professor, and since March 1994, he has been Adjunct Professor in the Department of Electrical Engineering of Catholic University of Pelotas. His interests include soft-switching techniques, dc/dc converters, and power factor correction techniques.



**Ivo Barbi** (M'78-SM'90) was born in Gaspar, Santa Catarina, Brazil, in 1949. He received the B.S. and M.S. degrees in electrical engineering from Federal University of Santa Catarina, Brazil, in 1973 and 1976, respectively, and the Ph.D. degree from the Polytechnic National Institute of Toulouse, France, in 1979.

He founded the Brazilian Power Electronics Society and the Power Electronics Institute of the Federal University of Santa Catarina, where he currently works as a Professor.

From 1992 to early 1996, Dr. Barbi was Associate Editor in the power converters area of the IEEE TRANSACTIONS ON INDUSTRIAL ELECTRONICS.